Received: 11 December 2019 | Revised: 19 March 2020 | Accepted: 27 March 2020

DOI: 10.1002/jms.4521

RESEARCH ARTICLE

Journal of MASS SPECTROMETRY WILEY

Energy-dependent normal and unusually large inverse chlorine kinetic isotope effects of simple chlorohydrocarbons in collision-induced dissociation by gas chromatography-electron ionization-tandem mass spectrometry

Caiming Tang[1] | Jianhua Tan[2] | Peilin Zhang[2] | Yujuan Fan[1,3] | Zhiqiang Yu[1] | Xianzhi Peng[1]

[1]State Key Laboratory of Organic Geochemistry, Guangzhou Instituteof Geochemistry, Chinese Academy of Sciences, Guangzhou, 510640, China

[2]Guangzhou Quality Supervision and Testing Institute, Guangzhou, 510110, China

[3]University of Chinese Academy of Sciences, Beijing, 100049, China

Correspondence
Caiming Tang, State Key Laboratory of Organic Geochemistry, Guangzhou Institute of Geochemistry, Chinese Academy of Sciences, Guangzhou 510640, China.
Email: caimingtang@gig.ac.cn

Funding information
National Natural Science Foundation of China, Grant/Award Number: 41603092

Abstract

Kinetic isotope effects (KIEs) occurring in mass spectrometry (MS) can provide in-depth insights into the fragmentation behaviors of compounds of interest in MS. Yet, the fundamentals of KIEs in collision-induced dissociation (CID) in tandem mass spectrometry (MS/MS) are unclear, and information about chlorine KIEs (Cl-KIEs) of organochlorines in MS is particularly scarce. This study investigated the Cl-KIEs of dichloromethane, trichloroethylene, and tetrachloroethylene during CID using gas chromatography-electron ionization triple-quadrupole MS/MS. Cl-KIEs were evaluated with MS signal intensities. All the organochlorines presented large inverse Cl-KIEs (<1, the departures of Cl-KIEs from 1 denote the magnitudes of Cl-KIEs), showing the largest magnitudes of 0.797, 0.910, and 0.892 at the highest collision energy (60 eV) for dichloromethane, trichloroethylene, and tetrachloroethylene, respectively. For dichloromethane, both intra-ion and inter-ion Cl-KIEs were studied, within the ranges of 0.820–1.020 and 0.797–1.016, respectively, showing both normal and inverse Cl-KIEs depending on collision energies. The observed Cl-KIEs generally declined from large normal to extremely large inverse values with increasing collision energies from 0 to 60 eV but were inferred to be independent of MS signal intensities. The Cl-KIEs are dominated by critical energies at low internal energies of precursor ions, resulting in normal Cl-KIEs; while at high internal energies, the Cl-KIEs are controlled by rotational barriers (or looseness/tightness of transition states), which lead to isotope-competitive reactions in dechlorination and thereby inverse Cl-KIEs. It is concluded that the Cl-KIEs may depend on critical energies, bond strengths, available internal energies, and transition state looseness/tightness. The findings of this study yield new insights into the fundamentals of Cl-KIEs of organochlorines during CID and may be conducive to elucidating the underlying mechanisms of KIEs in collision-induced and photo-induced reactions in the actual world.

KEYWORDS

chlorine kinetic isotope effects, chlorohydrocarbons, collision energy, collision-induced dissociation, electron ionization tandem mass spectrometry, isotope-competitive reactions

1 | INTRODUCTION

Kinetic isotope effects (KIEs) occurring in mass spectrometry (MS) have been extensively studied for quite a long time in terms of observations, theories, mechanisms, and applications,[1–4] which may provide in-depth insights into fragmentation behaviors of compounds of interest in MS. Large KIEs can occur during fragmentation in ionization source, metastable-ion decomposition in mass analyzer, and collision-induced dissociation (CID) in tandem mass spectrometry (MS/MS).[5–7] By means of MS, KIEs can be readily determined and applied to probing reaction mechanisms of molecules and ions in gas phase.[8–10] So far, most studies relevant to KIEs in MS focused on hydrogen/deuterium (H/D) KIEs,[5,11–13] whereas only a few concerned heavy-atom KIEs such as chlorine KIEs (Cl-KIEs).[14–16]

Cl-KIEs can take place in electron ionization-MS (EI-MS) during both ionization and metastable-ion dissociation.[17,18] In addition, some studies have reported the Cl-KIEs of some mono-chlorinated organic compounds,[19] chloroform,[20] tetrachloromethane,[21] dichloromethane (DCM),[22] metastable dichloromethane cation $[CH_2Cl_2]^{\bullet+}$,[23] and chloride adducts of some chlorinated/nonchlorinated organic compounds[14,16,20] taking place during CID in MS/MS. Both normal (>1) and inverse (<1) Cl-KIEs were observed in these studies with very large magnitudes in comparison with those during reactions in solution, and some mechanistic interpretations have been proposed for the Cl-KIEs. Zakett et al. pointed out that the magnitudes of Cl-KIEs of organochlorines were dependent on the internal energies and structures of ions.[19] Petersen et al. found large normal Cl-KIEs of chloroform during CID and concluded that the dechlorination reaction proceeded via two different pathways and the Cl-KIEs were symmetry-induced.[20] Additionally, Petersen et al. discovered extremely large normal Cl-KIEs of metastable $[CH_2Cl_2]^{\bullet+}$ in CID (Cl-KIE = 9) and concluded that the Cl-KIEs were determined by the predissociation rate and could be explained in light of vibrational overlap integrals.[23] Augusti et al. observed large normal and inverse Cl-KIEs of chloride adducts of aliphatic alcohols, benzaldehyde, and 2,4-pentanedione during CID[16] and deduced that the Cl-KIEs were triggered by differences of zero-point energies (ΔZPEs) between isotopomers, which was in agreement with the conclusions of Gozzo et al.[15] Extremely large inverse Cl-KIEs of $CHCl_4^-$ during CID were observed and inferred to be owing to the near-threshold centrifugal effect.[14] Probably because of the different ionization methods used (i.e., EI and chemical ionization) and different natures of the monitored ions (i.e., radical cations and chloride adduct anions) in these studies, different mechanistic interpretations for Cl-KIEs in CID from varied perspectives were presented. Yet, the relationships between Cl-KIEs in CID and internal energies of precursor ions have not been unraveled, let alone whether both normal and inverse Cl-KIEs of individual organochlorines can occur along with the variation of internal energies that depend on collision energies (CEs).

Herein, we conducted a systematic study to investigate the Cl-KIEs of chlorohydrocarbons in CID by gas chromatography electron ionization triple-quadrupole MS/MS (GC–MS/MS) using DCM, trichloroethylene (TCE), and tetrachloroethylene (PCE) as model compounds. By changing CEs within a relatively large range, the relationships between Cl-KIEs and internal energies were revealed. Theories in terms of quasi-equilibrium theory (QET) and isotope-competitive reactions were applied to interpreting mechanisms of the internal energy-dependent large normal and inverse Cl-KIEs of DCM. This study provides a new understanding on Cl-KIEs of organochlorines in CID and may shed light on Cl-KIEs of organochlorines in collision-induced and photo-induced dechlorination in the real world.

2 | MATERIALS AND METHODS

2.1 | Chemicals and materials

DCM (purity: 99.8%) was purchased from BCR International Trading Co., Ltd (California, USA), and TCE (purity: 99.0%) and PCE (purity: 99.0%) were bought from Dr. Ehrenstorfer (Augsburg, Germany). Solvent n-hexane was obtained from Merck Corp. (Darmstadt, Germany). All the chemicals were of chromatographic grade and used without further purification. The chemicals DCM, TCE, and PCE were accurately weighed and dissolved in n-hexane to prepare solutions at 1.0 mg/mL, which were further diluted with n-hexane to prepare injection solutions at 100.0 μg/mL. All the solutions were stored at −20°C condition prior to GC–MS/MS detection.

2.2 | GC–MS/MS measurement

The GC–MS/MS system consisted of an Agilent 7890B gas chromatograph and an Agilent 7000D triple quadrupole mass spectrometer (Agilent Technologies, Palo Alto, CA, USA). The chromatographic separation was conducted with an Agilent DB-INNOWAX capillary column (30 m × 0.25 mm, 0.25-μm thickness, Agilent Technologies). The temperature programs and other GC parameters are detailed in Table S1. The instrument control and data processing were performed with MassHunter Workstation (Agilent Technologies). The working solutions were directly injected onto the GC–MS/MS system with the injection volume of 1 μL, and splitless injection mode was adopted. At each instrumental condition, six replicated measurements were carried out.

The mass spectrometric working conditions and parameters for DCM are detailed as follows: EI source was used, and positive ions were monitored; EI energy was 45 eV (at this EI energy, high abundance of the molecular [precursor] ion could be obtained); ionization source temperature was 250°C; multiple reaction monitoring (MRM) mode was used for data acquisition; dwell time of each MRM transition was 25 ms; mass resolution was set at unit level (0.7 u) for both MS1 and MS2; collision gas was N_2 at the pressure of 10 psi; CEs were 0, 0.1, 0.2, 0.5, 1, 2, 3, 4, 5, 6, 8, 10, 12, 15, 20, 30, 40, 45, 50, and 60 eV. The working conditions and parameters of the tandem mass spectrometer for TCE and PCE are generally similar to those for DCM. Some specific mass spectrometric parameters for TCE and PCE are detailed as the following: The ionization source was maintained at

280°C; dwell time of each MRM transition was 30 ms; CEs were 0, 0.1, 0.2, 0.5, 1, 2, 5, 10, 15, 20, 30, 40, 45, 50, and 60 eV; solvent delay time was 3 min; scan window for TCE was 3–4.7 min and that for PCE was 4.7–12.7 min. The detailed information related to the MRM transitions is provided in Table 1, and the representative MRM chromatograms are shown in Figure S1.

In addition, we conducted product ion scan of $[CH_2{}^{35}Cl{}^{37}Cl]^{\bullet+}$ (*m/z* 86.0) of DCM using GC–MS/MS at the CEs of 0, 10, 12, 15, 20, 30, 40, 45, 50, and 60 eV with the scan range of *m/z* 10–100, in order to ascertain possible impact of the reaction $[CH_2{}^{35}Cl{}^{37}Cl]^{\bullet+} \rightarrow [C^{37}Cl]^+$ (*m/z* 86.0 → 49.0) on the measured intra-ion Cl-KIEs. All other GC–MS/MS parameters were identical to those applied to MRM experiment for DCM as described above. Because of the low resolving power, the mass spectrometer utilized in this study cannot differentiate $[CH_2{}^{35}Cl]^+$ (*m/z* 48.98395) and $[C^{37}Cl]^+$ (*m/z* 48.96535). As a result, the measured MS signal intensity of the MRM transition *m/z* 86.0 → 49.0 was actually the combined intensities of the reactions of $[CH_2{}^{35}Cl{}^{37}Cl]^{\bullet+} \rightarrow [CH_2{}^{35}Cl]^+$ and $[CH_2{}^{35}Cl{}^{37}Cl]^{\bullet+} \rightarrow [C^{37}Cl]^+$. The MS signal intensity ratios between *m/z* 47.0 ($[C^{35}Cl]^+$) and *m/z* 49.0 (the combination of $[CH_2{}^{35}Cl]^+$ and $[C^{37}Cl]^+$) were used to adjust the measured intra-ion Cl-KIEs of DCM. The measured inter-ion Cl-KIEs of DCM and intra-ion Cl-KIEs of TCE and PCE were not affected by the collision-induced dehydrogenation reactions losing two hydrogen atoms in principle.

2.3 | Data processing

Both intra-ion and inter-ion Cl-KIEs of DCM were evaluated of which the descriptions were detailed in our previous study.[17] Briefly, an intra-ion KIE occurs when a isotopologue ion give rise to two different product isotopologues by losing different isotopes, for example, $[CH_2{}^{35}Cl{}^{37}Cl]^{\bullet+} \rightarrow [CH_2{}^{37}Cl]^+$ versus $[CH_2{}^{35}Cl{}^{37}Cl]^{\bullet+} \rightarrow [CH_2{}^{35}Cl]^+$; an inter-ion KIE occurs when two isotopologue ions generate two product ions via two isotopically different fragmental pathways, for example, $[CH_2{}^{35}Cl_2]^{\bullet+} \rightarrow [CH_2{}^{35}Cl]^+$ versus $[CH_2{}^{37}Cl_2]^{\bullet+} \rightarrow [CH_2{}^{37}Cl]^+$. As none $[C^{35}Cl]^+$ (*m/z* 47.0) could be observed when CEs were ≤10 eV (Figure 1A,B), the intra-ion Cl-KIEs of DCM in the CE region of 0–10 eV were calculated with

$$KIE_{Intra\_0-10} = I_{86.0\rightarrow51.0}/I_{86.0\rightarrow49.0}, \quad (1)$$

where *I* denotes the MS signal intensities corresponding to the respective MRM transitions indicated by the subscripts, that is, *m/z* 86.0 → 51.0 and 86.0 → 49.0 (similarly hereinafter). Because $[C^{35}Cl]^+$ (*m/z* 47.0) started to appear when CEs were ≥12 eV, the intra-ion Cl-KIEs of DCM in the CE region of 12–60 eV were calculated with

$$KIE_{Intra\_12-60} = I_{86.0\rightarrow51.0}/[I_{86.0\rightarrow49.0} \times (1 - I_{47.0}/I_{49.0})], \quad (2)$$

where $I_{47.0}$ and $I_{49.0}$ denote the MS signal intensities of $[C^{35}Cl]^+$ (*m/z* 47.0) and $[CH_2{}^{35}Cl]^+$ (*m/z* 49.0) measured by product ion scan of $[CH_2{}^{35}Cl{}^{37}Cl]^{\bullet+}$ (*m/z* 86.0), respectively.

In addition, the inter-ion Cl-KIEs of DCM were calculated as follows:

$$KIE_{Inter} = I_{84.0\rightarrow49.0} \times R_{Cl}{}^2/I_{88.0\rightarrow51.0}, \quad (3)$$

where R_{Cl} is the corresponding chlorine isotope ratio of DCM calculated as follows:

TABLE 1 Collision-induced dissociation (CID) reactions and multiple reaction monitoring (MRM) transitions of dichloromethane (DCM), trichloroethylene (TCE), and tetrachloroethylene (PCE) by GC–MS/MS

Compound	CID reaction	*m/z* value of MRM transition	Number of lost ^{35}Cl atom	Number of lost ^{37}Cl atom
DCM	$[CH_2{}^{35}Cl_2]^{\bullet+} \rightarrow [CH_2{}^{35}Cl]^+$	84.0 → 49.0	1	0
	$[CH_2{}^{35}Cl_2]^{\bullet+} \rightarrow [CH_2{}^{35}Cl_2]^+$	84.0 → 84.0	0	0
	$[CH_2{}^{35}Cl{}^{37}Cl]^{\bullet+} \rightarrow [CH_2{}^{35}Cl]^+$	86.0 → 49.0	0	1
	$[CH_2{}^{35}Cl{}^{37}Cl]^{\bullet+} \rightarrow [CH_2{}^{37}Cl]^+$	86.0 → 51.0	1	0
	$[CH_2{}^{35}Cl{}^{37}Cl]^{\bullet+} \rightarrow [CH_2{}^{35}Cl{}^{37}Cl]^+$	86.0 → 86.0	0	0
	$[CH_2{}^{37}Cl_2]^{\bullet+} \rightarrow [CH_2{}^{37}Cl]^+$	88.0 → 51.0	0	1
	$[CH_2{}^{37}Cl_2]^{\bullet+} \rightarrow [CH_2{}^{37}Cl_2]^+$	88.0 → 88.0	0	0
TCE	$[C_2H{}^{35}Cl_2{}^{37}Cl]^{\bullet+} \rightarrow [C_2H\ {}^{35}Cl_2]^+$	131.9 → 94.9	0	1
	$[C_2H{}^{35}Cl_2{}^{37}Cl]^{\bullet+} \rightarrow [C_2H\ {}^{35}Cl{}^{37}Cl]^+$	131.9 → 96.9	1	0
	$[C_2H{}^{35}Cl{}^{37}Cl_2]^{\bullet+} \rightarrow [C_2H\ {}^{35}Cl{}^{37}Cl]^+$	133.9 → 96.9	0	1
	$[C_2H{}^{35}Cl{}^{37}Cl_2]^{\bullet+} \rightarrow [C_2H\ {}^{37}Cl_2]^+$	133.9 → 98.9	1	0
PCE	$[C_2{}^{35}Cl_3{}^{37}Cl]^{\bullet+} \rightarrow [C_2{}^{35}Cl_3]^+$	165.9 → 128.9	0	1
	$[C_2{}^{35}Cl_3{}^{37}Cl]^{\bullet+} \rightarrow [C_2{}^{35}Cl_2{}^{37}Cl]^+$	165.9 → 130.9	1	0
	$[C_2{}^{35}Cl_2{}^{37}Cl_2]^{\bullet+} \rightarrow [C_2{}^{35}Cl_2]^+$	167.9 → 93.9	0	2
	$[C_2{}^{35}Cl_2{}^{37}Cl_2]^{\bullet+} \rightarrow [C_2{}^{37}Cl_2]^+$	167.9 → 97.9	2	0
	$[C_2{}^{35}Cl_2{}^{37}Cl_2]^{\bullet+} \rightarrow [C_2{}^{35}Cl_2{}^{37}Cl]^+$	167.9 → 130.9	0	1
	$[C_2{}^{35}Cl_2{}^{37}Cl_2]^{\bullet+} \rightarrow [C_2{}^{35}Cl{}^{37}Cl_2]^+$	167.9 → 132.9	1	0

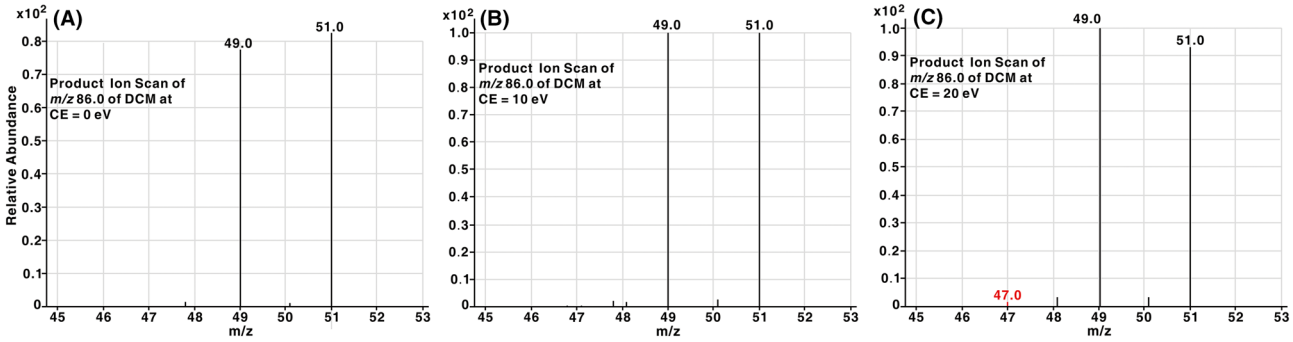

FIGURE 1 Representative product ion scan spectra of $[CH_2{}^{35}Cl{}^{37}Cl]^{\bullet+}$ (*m/z* 86.0) of dichloromethane (DCM) at collision energies (CEs) of A, 0, B, 10, and C, 20 eV by GC–MS/MS. The intensity discrepancies between $[CH_2{}^{35}Cl]^+$ (*m/z* 49.0) and $[CH_2{}^{37}Cl]^+$ (*m/z* 51.0) point to the intra-ion chlorine kinetic isotope effects (Cl-KIEs) of DCM. The ion $[C^{35}Cl]^+$ (*m/z* 47.0) could be observed when CEs were higher than 12 eV, such as at (C) 20 eV

$$R_{Cl} = \frac{I_{88.0\rightarrow88.0} \times 2 + I_{86.0\rightarrow86.0}}{I_{84.0\rightarrow84.0} \times 2 + I_{86.0\rightarrow86.0}}, \quad (4)$$

which is derived from previously reported schemes of isotope-ratio calculation.[17,24,25] The calculation schemes for the intra-ion Cl-KIEs of TCE and PCE, similar to that of DCM, are detailed in the Supporting Information. All these calculation schemes originate from the literature.[1] The total MS signal intensity of each MRM transition within the retention time range of each chromatographic peak was exported from the corresponding raw data file and applied to Cl-KIE calculation. Prior to exporting MS signal intensities, background subtraction was conducted by subtracting the baseline signal intensities at both ends of each peak from the peak. Data from six replicated injections were used to calculate the average MS signal intensities and Cl-KIEs along with their standard deviations (1σ).

2.4 | Statistical analysis

Statistical analysis was conducted with SPSS Statistics 19.0 (IBM Inc., Armonk, USA) and Origin 9 (OriginLab Corp., Northampton, USA). Independent-samples *T* test and paired-samples *T* test, performed with SPSS, were applied to examining the differences among Cl-KIEs at different CEs, and different types of Cl-KIEs by determining *p* values (two-tailed) ≤ 0.01 for significance. Linear and nonlinear regressions, implemented by Origin, were employed to reveal the relationships between measured Cl-KIEs and parameters/factors of interest (i.e., CEs and MS signal intensities).

2.5 | Computational methods

Computational chemistry studies were performed with Gaussian 09 program package,[26] for investigating the gas-phase dechlorination reactions of PCE in CID process. Density functional theory (DFT) calculations were carried out by the Becke three-parameter hybrid exchange functional and Lee-Yang-Parr correlation functional (B3LYP) with the 6-311G(d) basis set.[27,28] Frequency calculations were conducted at the same level of theory to attain the values of enthalpy, entropy, Gibbs free energy, and zero-point energy (ZPE), to confirm the nature of stationary points on potential energy surface for the minima and transition states (TSs).

3 | RESULTS AND DISCUSSION

3.1 | Validity of measured Cl-KIEs

In this study, we aimed to unravel the relationships between Cl-KIEs and internal energies of precursor ions during CID in MS/MS. The measured Cl-KIEs were critical to implement the revelation of the relationships, and therefore, it was crucial to confirm their validity prior to application. As shown in Figure 1A,C, the intensity discrepancies between $[CH_2{}^{35}Cl]^+$ (*m/z* 49.0) and $[CH_2{}^{37}Cl]^+$ (*m/z* 51.0) visually indicate the differentiable extents of the two branch reactions.

Crosstalk during MRM might be a factor capable of affecting the validity of measured Cl-KIEs. For DCM, seven MRM transitions were monitored (Table 1). Both the precursor ions $[CH_2{}^{35}Cl_2]^{\bullet+}$ (*m/z* 84.0) and $[CH_2{}^{35}Cl{}^{37}Cl]^{\bullet+}$ (*m/z* 86.0) can give rise to the product ion $[CH_2{}^{35}Cl]^+$, and both the precursor ions $[CH_2{}^{35}Cl{}^{37}Cl]^{\bullet+}$ and $[CH_2{}^{37}Cl_2]^{\bullet+}$ (*m/z* 88.0) can yield the product ion $[CH_2{}^{37}Cl]^+$. As a consequence, if crosstalk presents, the precursor ion $[CH_2{}^{35}Cl_2]^{\bullet+}$ could influence the monitoring of the MRM transition of $[CH_2{}^{35}Cl{}^{37}Cl]^{\bullet+} \rightarrow [CH_2{}^{35}Cl]^+$ (*m/z* 86.0 → 49.0) by enhancing the MS signal intensity. On the other hand, the precursor ion $[CH_2{}^{35}Cl{}^{37}Cl]^{\bullet+}$ could enhance the MS signal intensity of the transition of $[CH_2{}^{37}Cl_2]^{\bullet+} \rightarrow [CH_2{}^{37}Cl]^+$ (*m/z* 88.0 → 51.0). We accordingly conducted an experiment by monitoring the transitions of *m/z* $[CH_2{}^{35}Cl{}^{37}Cl]^{\bullet+} \rightarrow [CH_2{}^{35}Cl]^+$ and $[CH_2{}^{35}Cl{}^{37}Cl]^{\bullet+} \rightarrow [CH_2{}^{37}Cl]^+$ (*m/z* 86.0 → 51.0) exclusively and another experiment monitoring the transitions of $[CH_2{}^{35}Cl_2]^{\bullet+} \rightarrow [CH_2{}^{35}Cl]^+$ (*m/z* 84.0 → 49.0) and $[CH_2{}^{37}Cl_2]^{\bullet+} \rightarrow [CH_2{}^{37}Cl]^+$ only. As shown in Figure 2, Cl-KIEs obtained by monitoring all MRM transitions (combined scan) were very close to those by monitoring the transitions used for determining intra-ion and inter-

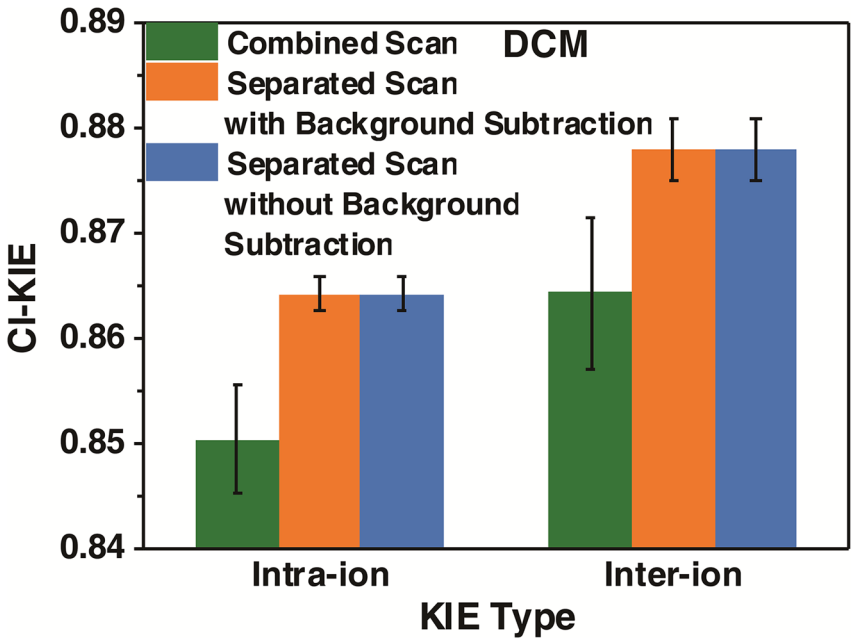

FIGURE 2 Intra-ion and inter-ion Cl-KIEs of DCM measured with the combined scan and separated scans with and without background subtraction. Combined scan: monitoring all MRM transitions of DCM; separated scans: monitoring merely *m/z* 86.0 → 49.0 ($[CH_2{}^{35}Cl^{37}Cl]^{\bullet+} \rightarrow [CH_2{}^{35}Cl]^+$) and 86.0 → 51.0 ($[CH_2{}^{35}Cl^{37}Cl]^{\bullet+} \rightarrow [CH_2{}^{37}Cl]^+$) or only *m/z* 84.0 → 49.0 ($[CH_2{}^{35}Cl_2]^{\bullet+} \rightarrow [CH_2{}^{35}Cl]^+$) and 88.0 → 51.0 ($[CH_2{}^{37}Cl_2]^{\bullet+} \rightarrow [CH_2{}^{37}Cl]^+$). The CE was set at 45 eV. Error bars represent the standard deviations (1σ, *n* = 6, the same below)

ion Cl-KIEs separately (separated scan). This result demonstrates that the crosstalk could not impact the determination of Cl-KIEs or might not be present in the instrumental analysis in this study.

In this study, background subtraction was carried out before exporting MS signal intensity, which might be another issue affecting the validity of measured Cl-KIEs. Background subtraction might take away slight real signal intensities from MRM transitions. And transitions with lower theoretical relative abundances were speculated to be affected by background subtraction more significantly in contrast to transitions with higher relative abundances. If so, the inter-ion Cl-KIEs obtained with background subtraction should be higher than those without background subtraction. However, as illustrated in Figure 2, the inter-ion Cl-KIEs obtained with and without subtraction were almost identical (p = 0.9), which demonstrates that the background subtraction had no effect on the measured Cl-KIEs. Ultimately, the validity of measured KIEs was accordingly confirmed.

3.2 | Evaluation of impacts of further dechlorination of product ions on measured Cl-KIEs

In this study, because the lost Cl atoms during CID cannot be detected, we thus detected the specific product ions and used their signal intensities to calculate Cl-KIEs. These product ions contain at least one Cl atom, which might be subjected to further dechlorination during CID or metastable-ion dissociation. Cl-KIEs are anticipated to be present in the further dechlorination reactions, therefore maybe affecting the measured Cl-KIEs. As a result, the correlations between Cl-KIEs and CEs attained in this study need scrutiny in terms of the influence from further dechlorination reactions of product ions. We use DCM as an exemplary compound to elucidate the influence and take the intra-ion Cl-KIEs into consideration at first. The intra-ion Cl-KIEs were derived from the reactions $[CH_2{}^{35}Cl^{37}Cl]^{\bullet+} \rightarrow [CH_2{}^{37}Cl]^+$ and $[CH_2{}^{35}Cl^{37}Cl]^{\bullet+} \rightarrow [CH_2{}^{35}Cl]^+$. As generally expected, a reaction losing a ^{35}Cl atom is faster than that losing a ^{37}Cl atom, that is, $k_{35Cl} > k_{37Cl}$ or Cl-KIE > 1. We hypothesize that the reaction of $[CH_2Cl_2]^{\bullet+} \rightarrow [CH_2Cl]^+$ exhibits a Cl-KIE > 1, then the further dechlorination reaction $[CH_2Cl^+ \rightarrow CH_2]^+$ should present a Cl-KIE higher than 1 also. Because the primary Cl-KIE was measured as the MS signal intensity ratio of $[CH_2{}^{35}Cl^{37}Cl]^{\bullet+} \rightarrow [CH_2{}^{37}Cl]^+$ to $[CH_2{}^{35}Cl^{37}Cl]^{\bullet+} \rightarrow [CH_2{}^{35}Cl]^+$, the abundance of $[CH_2{}^{37}Cl]^+$ should be higher than that of $[CH_2{}^{35}Cl]^+$. When taking the further dechlorination into account, more amount of $[CH_2{}^{35}Cl]^+$ is further dechlorinated than that of $[CH_2{}^{37}Cl]^+$. Therefore, the measured Cl-KIEs should be higher than the real values during specific dechlorination reactions, which means the further dechlorination reactions fortify the measured Cl-KIEs. As a result, in this study, the measured Cl-KIEs (mainly under unity) could not be caused by the further Cl-KIEs that were higher than unity, and thus, the measured Cl-KIEs lower than unity were really existent.

From the other side, we hypothesize that the primary and the further inter-ion Cl-KIEs were >1. The inter-ion Cl-KIEs were derived from the reactions of $[CH_2{}^{35}Cl_2]^{\bullet+} \rightarrow [CH_2{}^{35}Cl]^+$ and $[CH_2{}^{37}Cl_2]^{\bullet+} \rightarrow [CH_2{}^{37}Cl]^+$. We postulate that the amounts of the ions $[CH_2{}^{35}Cl_2]^{\bullet+}$ and $[CH_2{}^{37}Cl_2]^{\bullet+}$ are identical, then the abundance of the product ion $CH_2{}^{35}Cl^+$ prior to further dechlorination is higher than that of $[CH_2{}^{37}Cl]^+$. Whereas $[CH_2{}^{35}Cl]^+$ is more likely to lose ^{35}Cl than $[CH_2{}^{37}Cl]^+$ to lose ^{37}Cl according to the hypothesis. Therefore, the primary and the further inter-ion Cl-KIEs make contribution to the measured Cl-KIEs for individual specific dechlorination reactions from opposite directions. In this context, it is possible that the measured Cl-KIEs can be either higher or lower than unity, depending on the magnitudes of the primary and the further inter-ion Cl-KIEs and the extents of dechlorination reactions. According to the QET and ZPE theory, low internal energy of ions can enhance KIEs. However,

the magnitudes (deviations from unity) of measured inter-ion Cl-KIEs (under unity) were increasing as the CEs increased from 6 to 60 eV. This observation indicates that the measured inter-ion Cl-KIEs were not likely triggered by the further Cl-KIEs in dissociation of product ions, particularly for those measured in the high energy region.

3.3 | Observed relationships between Cl-KIEs and CEs

Both intra-ion and inter-ion Cl-KIEs of DCM during CID in GC-EI-MS/MS were investigated in this study. The intra-ion Cl-KIEs were derived from the reactions of $[CH_2{}^{35}Cl{}^{37}Cl]^{\bullet+} \rightarrow [CH_2{}^{37}Cl]^+$ versus $[CH_2{}^{35}Cl{}^{37}Cl]^{\bullet+} \rightarrow [CH_2{}^{35}Cl]^+$, and the inter-ion Cl-KIEs were derived from the reactions of $[CH_2{}^{35}Cl_2]^{\bullet+} \rightarrow [CH_2{}^{35}Cl]^+$ versus $[CH_2{}^{37}Cl_2]^{\bullet+} \rightarrow [CH_2{}^{37}Cl]^+$. The rate constants corresponding to the reactions by losing ^{35}Cl or ^{37}Cl atoms are denoted as k_{35Cl} and k_{37Cl}, respectively, and the Cl-KIE is equal to k_{35Cl}/k_{37Cl}. The validity of the measured Cl-KIEs was confirmed in terms of direct observation of signal intensity differences (Figure 1A,C), crosstalk effects, and background subtraction influences (Figure 2), and the Cl-KIEs were deduced to be not attributable to further dechlorination reactions of product ions. In view of the impact of collision-induced dehydrogenation reactions losing two hydrogen atoms on the measured intra-ion Cl-KIEs of DCM in the CE region of 12–60 eV (Figure 1C), the corresponding Cl-KIEs were adjusted by the MS signal intensity ratios of *m/z* 47 ($[C^{35}Cl]^+$) to *m/z* 49 (the combination of $[CH_2{}^{35}Cl]^+$ and $[C^{37}Cl]^+$) as indicated in Equation 2.

As shown in Figure 3, both the intra-ion and inter-ion Cl-KIEs generally declined as the CEs increased from 0 to 60 eV. The highest intra-ion and inter-ion Cl-KIEs were 1.020 ± 0.001 and 1.016 ± 0.004, respectively, and the lowest were 0.820 ± 0.014 and 0.797 ± 0.023, respectively (Table S2). We divide the CEs set for detecting DCM into two regions, namely, a low energy region (0–12 eV) and a high energy region (15–60 eV). In the low energy region, the intra-ion Cl-KIEs were significantly higher than unity, where $k_{35Cl} = k_{37Cl}$ ($p \leq 0.003$) with the CEs ≤ 2 eV, but were significantly lower than unity when the CEs were ≥3 eV ($p \leq 0.001$, Figure 3A). In addition, all the intra-ion Cl-KIEs were significantly lower than unity in the high energy region ($p < 0.001$, Figure 3B). The inter-ion Cl-KIEs were higher than unity when the CEs were ≤8 eV ($p \leq 0.006$) and lower than unity as the CEs were ≥12 eV ($p \leq 0.01$, Figure 3C).

The correlations between Cl-KIEs and CEs can be well fitted with exponential functions ($R^2 \geq 0.939$, Figure 3). It is noteworthy that the fitted curves for the intra-ion Cl-KIEs were concave in the low energy region but convex in the high energy region, manifesting a decelerating decline of Cl-KIEs with the CEs from 0 to 12 eV and an accelerating decline with the CEs from 15 to 60 eV (Figure 3A,B). This observation may imply different mechanisms of intra-ion Cl-KIEs and CID in the low and the high energy regions. On the other hand, the inter-ion KIEs generally exhibited a convex exponential curve from 0 to 60 eV, demonstrating an accelerating decline in the whole energy region (Figure 3C).

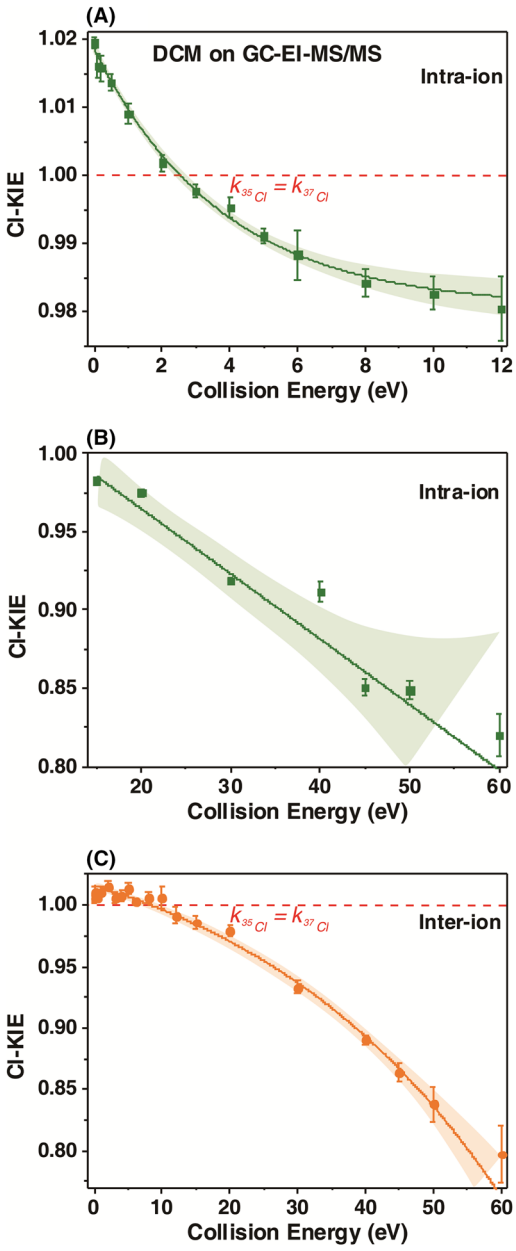

FIGURE 3 Measured Cl-KIEs of DCM during collision-induced dissociation (CID) at different CEs. The CEs are divided into two regions, that is, a low energy region (0–12 eV) and a high energy region (15–60 eV). Note, (A) and (B): intra-ion Cl-KIEs measured at the low and the high energy regions, respectively; (C): inter-ion Cl-KIEs measured at the whole energy region (0–60 eV); k_{35Cl} and k_{37Cl} indicate the rate constants corresponding to the dechlorination reactions by losing ^{35}Cl and ^{37}Cl atoms, respectively; solid curves represent exponential regressions, and shaded areas indicate the corresponding 95% confidence intervals (similarly hereinafter); the fitted functions for intra-ion Cl-KIEs versus CEs were (A) $y = 0.981 + 0.038\exp(-0.266x)$ ($R^2 = 0.994$) and (B) $y = 16.089 - 15.041\exp(2.747 \times 10^{-4}x)$ ($R^2 = 0.939$), respectively, and that for inter-ion Cl-KIEs versus CEs was (C) $y = 1.083 - 0.067\exp(0.026x)$ ($R^2 = 0.985$); the decimals of the fitting parameters were displayed according to the respective standard deviations (1σ, similarly hereinafter)

Because we could not obtain the exact relative abundances of $[CH_2{}^{35}Cl_2]^{\bullet+}$ and $[CH_2{}^{37}Cl_2]^{\bullet+}$ that transformed into $[CH_2{}^{35}Cl]^+$ and $[CH_2{}^{37}Cl]^+$, respectively, we thus determined the molecular chlorine isotope ratios to adjust the measured MS signal intensity ratios of $[CH_2{}^{35}Cl_2]^{\bullet+} \rightarrow [CH_2{}^{35}Cl]^+$ to $[CH_2{}^{37}Cl_2]^{\bullet+} \rightarrow [CH_2{}^{37}Cl]^+$ for attaining the rough inter-ion Cl-KIEs (Equations 3 and 4). As shown in Figure S2, the raw intensity ratios between $[CH_2{}^{35}Cl_2]^{\bullet+} \rightarrow [CH_2{}^{35}Cl]^+$ and $[CH^{2}{}^{37}Cl_2]^{\bullet+} \rightarrow [CH_2{}^{37}Cl]^+$ generally declined along with the CEs from 0 to 60 eV, which coincides well with the correlations between the inter-ion KIEs and CEs as illustrated in Figure 3C. Therefore, the measured inter-ion Cl-KIEs can correctly reflect the relationships between the exact inter-ion Cl-KIEs and CEs, even though the measured inter-ion Cl-KIEs were approximate values.

In addition to DCM, TCE and PCE were also used as model compounds to investigate Cl-KIEs during CID. Because of the low abundances of the isotopologues whose chlorine atoms are merely ^{37}Cl, inter-ion Cl-KIEs were not studied. In addition, because TCE and PCE have more than two Cl atoms, the degrees of freedom for losing Cl atoms should be taken into account (Equations S1–S3). As shown in Figure 4, the measured Cl-KIEs linearly decreased as the CEs increased from 0 to 60 eV. The highest Cl-KIEs derived from the reactions of $[C_2H^{35}Cl_2{}^{37}Cl]^{\bullet+} \rightarrow [C_2H^{35}Cl^{37}Cl]^+$ versus $[C_2H^{35}Cl_2{}^{37}Cl]^{\bullet+} \rightarrow [C_2H^{35}Cl_2]^+$, and $[C_2H^{35}Cl^{37}Cl_2]^{\bullet+} \rightarrow [C_2H^{37}Cl_2]^+$ versus $[C_2H^{35}Cl^{37}Cl_2]^{\bullet+} \rightarrow [C_2H^{35}Cl^{37}Cl]^+$ for TCE were 0.999 ± 0.003 and 0.992 ± 0.007, respectively, and the lowest were 0.910 ± 0.005 and 0.926 ± 0.009, respectively (Figure 4A and Table S3). As for PCE, the highest Cl-KIEs derived from the reactions of $[C_2{}^{35}Cl_3{}^{37}Cl]^{\bullet+} \rightarrow [C_2{}^{35}Cl_2{}^{37}Cl]^+$ versus $[C_2{}^{35}Cl_3{}^{37}Cl]^{\bullet+} \rightarrow [C_2{}^{35}Cl_3]^+$ and $[C_2{}^{35}Cl_2{}^{37}Cl_2]^{\bullet+} \rightarrow [C_2{}^{35}Cl^{37}Cl_2]^+$ versus $[C_2{}^{35}Cl_2{}^{37}Cl_2]^{\bullet+} \rightarrow [C_2{}^{35}Cl_2{}^{37}Cl]^+$ were 0.982 ± 0.005 and 0.986 ± 0.004, respectively, and the lowest were 0.905 ± 0.010 and 0.892 ± 0.005, respectively (Figure 4B and Table S3). The fitted lines for the correlations between Cl-KIEs and CEs are very similar, showing indistinguishable Cl-KIEs of each compound at individual CEs ($p \geq 0.04$). Besides the Cl-KIEs of PCE derived from $[C_2{}^{35}Cl_2{}^{37}Cl_2]^{\bullet+} \rightarrow [C_2{}^{35}Cl^{37}Cl_2]^+$ versus $[C_2{}^{35}Cl_2{}^{37}Cl_2]^{\bullet+} \rightarrow [C_2{}^{35}Cl_2{}^{37}Cl]^+$ by losing one Cl atom, the Cl-KIEs derived from $[C_2{}^{35}Cl_2{}^{37}Cl_2]^{\bullet+} \rightarrow [C_2{}^{37}Cl_2]^+$ versus $[C_2{}^{35}Cl_2{}^{37}Cl_2]^{\bullet+} \rightarrow [C_2{}^{35}Cl_2]^+$ by losing two Cl atoms were also investigated with the CEs from 20 to 60 eV (Table 1). As illustrated in Figure 4C, the Cl-KIEs derived from the reaction by losing one Cl atom were significantly lower than those from the reaction by losing two Cl atoms ($p = 5 \times 10^{-6}$). It is worth of noting that the Cl-KIE derived from the reaction losing two Cl atoms at CE of 20 eV exceeded unity with statistical significance (1.016 ± 0.006, $p = 0.01$) and that at 30 eV was very close to unity (0.999 ± 0.008, $p = 0.2$). Nevertheless, other Cl-KIEs of PCE were all under unity.

3.4 | Observed relationships between Cl-KIEs and MS signal intensities

For revealing the in-depth mechanisms of Cl-KIEs during CID, correlations between Cl-KIEs and MS signal intensities were investigated. As shown in Figure 5A, in the low energy region, the Cl-KIEs of DCM had

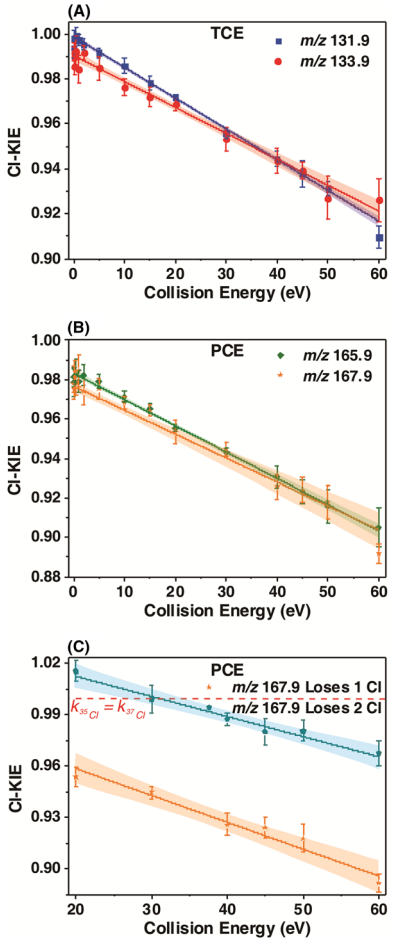

FIGURE 4 Measured Cl-KIEs of trichloroethylene (TCE) and tetrachloroethylene (PCE) during CID at different CEs. (A): The Cl-KIEs of TCE correspond to the reactions of $[C_2H^{35}Cl_2{}^{37}Cl]^{\bullet+} \rightarrow [C_2H^{35}Cl^{37}Cl]^+$ (*m/z* 131.9 → 96.9) versus $[C_2H^{35}Cl_2{}^{37}Cl]^{\bullet+} \rightarrow [C_2H\ {}^{35}Cl_2]^+$ (*m/z* 131.9 → 94.9) and $[C_2H^{35}Cl^{37}Cl_2]^{\bullet+} \rightarrow [C_2H\ {}^{37}Cl_2]^+$ (*m/z* 133.9 → 98.9) vs. $[C_2H^{35}Cl^{37}Cl_2]^{\bullet+} \rightarrow [C_2H^{35}Cl^{37}Cl]^+$ (*m/z* 133.9 → 96.9); (B): The Cl-KIEs of PCE correspond to the reactions of $[C_2{}^{35}Cl_3{}^{37}Cl]^{\bullet+} \rightarrow [C_2{}^{35}Cl_2{}^{37}Cl]^+$ (*m/z* 165.9 → 130.9) versus $[C_2{}^{35}Cl_3{}^{37}Cl]^{\bullet+} \rightarrow [C_2{}^{35}Cl_3]^+$ (*m/z* 165.9 → 128.9) and $[C_2{}^{35}Cl_2{}^{37}Cl_2]^{\bullet+} \rightarrow [C_2{}^{35}Cl^{37}Cl_2]^+$ (*m/z* 167.9 → 132.9) versus $[C_2{}^{35}Cl_2{}^{37}Cl_2]^{\bullet+} \rightarrow [C_2{}^{35}Cl_2{}^{37}Cl]^+$ (*m/z* 167.9 → 130.9); (C): The Cl-KIEs of PCE correspond to the reactions of $[C_2{}^{35}Cl_2{}^{37}Cl_2]^{\bullet+} \rightarrow [C_2{}^{35}Cl^{37}Cl_2]^+$ versus $[C_2{}^{35}Cl_2{}^{37}Cl_2]^{\bullet+} \rightarrow [C_2{}^{35}Cl_2{}^{37}Cl]^+$ and $[C_2{}^{35}Cl_2{}^{37}Cl_2]^{\bullet+} \rightarrow [C_2{}^{37}Cl_2]^+$ (*m/z* 167.9 → 97.9) versus $[C_2{}^{35}Cl_2{}^{37}Cl_2]^{\bullet+} \rightarrow [C_2{}^{35}Cl_2]^+$ (*m/z* 167.9 → 93.9) in the CE region of 20–60 eV; solid lines denote linear regressions; the fitted functions for Cl-KIEs versus CEs of the reactions of $[C_2H^{35}Cl_2{}^{37}Cl]^{\bullet+} \rightarrow [C_2H\ {}^{35}Cl^{37}Cl]^+$ versus $[C_2H^{35}Cl_2{}^{37}Cl]^{\bullet+} \rightarrow [C_2H\ {}^{35}Cl_2]^+$, $[C_2H^{35}Cl^{37}Cl_2]^{\bullet+} \rightarrow [C_2H^{37}Cl_2]^+$ versus $[C_2H^{35}Cl^{37}Cl_2]^{\bullet+} \rightarrow [C_2H^{35}Cl^{37}Cl]^+$, $[C_2{}^{35}Cl_3{}^{37}Cl]^{\bullet+} \rightarrow [C_2{}^{35}Cl_2{}^{37}Cl]^+$ versus $[C_2{}^{35}Cl_3{}^{37}Cl]^{\bullet+} \rightarrow [C_2{}^{35}Cl_3]^+$, $[C_2{}^{35}Cl_2{}^{37}Cl_2]^{\bullet+} \rightarrow [C_2{}^{35}Cl^{37}Cl_2]^+$ versus $[C_2{}^{35}Cl_2{}^{37}Cl_2]^{\bullet+} \rightarrow [C_2{}^{35}Cl_2{}^{37}Cl]^+$ (0–60 eV), $[C_2{}^{35}Cl_2{}^{37}Cl_2]^{\bullet+} \rightarrow [C_2{}^{35}Cl^{37}Cl_2]^+$ versus $[C_2{}^{35}Cl_2{}^{37}Cl_2]^{\bullet+} \rightarrow [C_2{}^{35}Cl_2{}^{37}Cl]^+$ (20–60 eV), and $[C_2{}^{35}Cl_2{}^{37}Cl_2]^{\bullet+} \rightarrow [C_2{}^{37}Cl_2]^+$ versus $[C_2{}^{35}Cl_2{}^{37}Cl_2]^{\bullet+} \rightarrow [C_2{}^{35}Cl_2]^+$ were $y = 0.999–0.001x$ ($R^2 = 0.996$), $y = 0.990–0.001x$ ($R^2 = 0.979$), $y = 0.983–0.001x$ ($R^2 = 0.990$), $y = 0.977–0.001x$ ($R^2 = 0.948$), $y = 0.990–0.002x$ ($R^2 = 0.963$), and $y = 1.036–0.001x$ ($R^2 = 0.958$), respectively

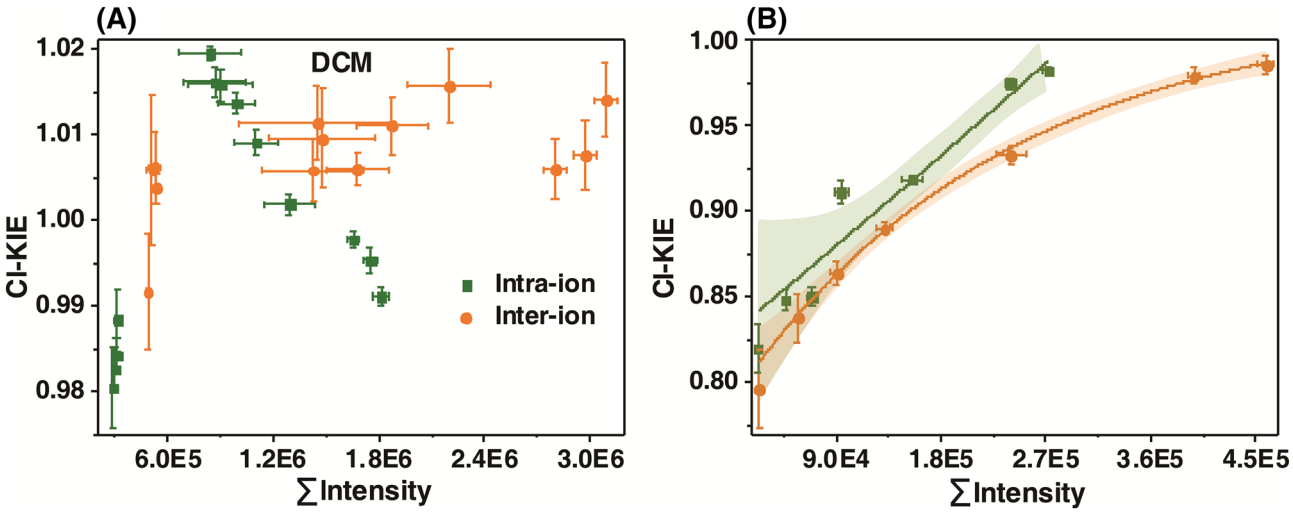

FIGURE 5 Correlations between Cl-KIEs and MS signal intensities of DCM obtained at different CEs. Note, (A): correlations at the low energy region (0–12 eV); (B): correlations at the high energy region (15–60 eV). ∑Intensity for intra-ion Cl-KIEs is the sum of the MS signal intensities of $[CH_2{}^{35}Cl{}^{37}Cl]^{\bullet+} \rightarrow [CH_2{}^{37}Cl]^+$ and $[CH_2{}^{35}Cl{}^{37}Cl]^{\bullet+} \rightarrow [CH_2{}^{35}Cl]^+$; ∑Intensity for inter-ion Cl-KIEs is the sum of the MS signal intensities of $[CH_2{}^{35}Cl_2]^{\bullet+} \rightarrow [CH_2{}^{35}Cl]^+$ and $[CH_2{}^{37}Cl_2]^{\bullet+} \rightarrow [CH_2{}^{37}Cl]^+$ for inter-ion Cl-KIEs; the fitted functions for intra-ion Cl-KIEs versus ∑Intensities and inter-ion Cl-KIEs versus ∑Intensities in the high energy region (B) were $y = -0.918 + 1.747\exp(3.201 \times 10^{-7}x)$ ($R^2 = 0.950$) and $y = 1.019 - 0.229\exp(-4.313 \times 10^{-6}x)$ ($R^2 = 0.996$), respectively

no relationship with the MS signal intensities. However, in the high energy region, the Cl-KIEs showed a general increase along with the increasing intensities ($R^2 \geq 0.950$, Figure 5B). This result indicates that there was no necessary connection between the Cl-KIEs and MS signal intensities. In addition, we plotted the MS signal intensities versus CEs and found the intensities increased as the CEs increased from 0 to 5 eV and decreased with the CEs from 6 to 60 eV (Figure S3). This observation indicates that the MS signal intensities were CE-dependent, just as the Cl-KIEs, but their CE-dependent variation modes were different (Figure 3 and Figure S3). Similar conclusions can also be drawn from the data of TCE and PCE (Figures S4 and S5). Therefore, although the MS signal intensities and Cl-KIEs were all CE-dependent, they had no necessary relationship. Accordingly, we can further infer that the Cl-KIEs occurring during CID are independent of injection concentrations and volumes of compounds and relative abundances of isotopologues.

3.5 | Computational results

The potential energy surface for the dechlorination reactions of PCE in CID process on GC-EI-MS/MS was obtained by DFT calculation. The potential barrier for the first dechlorination reaction $[C_2Cl_4]^{\bullet+} \rightarrow [C_2Cl_3]^+ + Cl^{\bullet}$ was 283.3 kJ/mol, and the enthalpy change was 233.9 kJ/mol (Figure 6). The length of the stretched C–Cl bond (C–Cl) of the TS of this reaction was 2.986 Å, shown as TS1 in Figure 6. With regard to the second dechlorination reaction $[C_2Cl_3]^+ \rightarrow [C_2Cl_2]^+ + Cl^{\bullet}$, the reaction energy barrier was 304.6 kJ/mol, and the enthalpy change was 219.2 kJ/mol. The TS of the second dechlorination reaction (TS2) possessed a C–Cl bond of 5.469 Å, which was much longer than that of TS1 (Figure 6).

3.6 | Mechanistic interpretation

Normal KIEs (>1) in MS are relatively easy to explain, because many studies have reported relevant observations and theoretical interpretations.[14,29] The normal KIEs can be successfully explained by the QET and ZPE theory.[1,30–33] The critical energy (E_0)[34] of an ion involving a bond with a light isotope is lower than that of the ion with a heavy isotope. Thus, the lighter isotopomer loses the light isotope more quickly than the heavier to lose the heavy isotope, presenting a normal KIE (>1). When internal energies of ions are near the critical energies of fragmentation reactions involving isotope atoms, the KIEs can be staggeringly large.[1] The measured normal Cl-KIEs of DCM in this study were in this scenario, showing decreasing tendencies from relatively large normal Cl-KIEs (1.020 ± 0.001) to approximate unity with the CEs from 0 to 3 eV (Figure 3). It is noteworthy that in this study, we could not directly explore the relationships between Cl-KIEs and internal energies of precursor ions but indirectly elucidate the relationships by revealing those between the measured Cl-KIEs and CEs. It is rational that the internal energies are CE-dependent and increasing as CEs increase, if not in linear correlations. Therefore, the correlations between the measured Cl-KIEs and CEs could to some extent reflect the actual relationships between the Cl-KIEs and internal energies.

On the other hand, inverse KIEs (<1) occurring in MS are very challenging to interpret, and only very limited studies have reported the observations and putative mechanisms of inverse KIEs.[14,20] Green et al. studied the inverse Cl-KIEs of chlorine adducts of three simple chloroalkanes in CID by losing Cl^- in MS/MS and found that the Cl-KIE of chloroform/Cl^- was extremely large and that of DCM/Cl^- was 0.90.[14] The authors concluded that the observed inverse Cl-KIEs during CID were attributable to the near-threshold dissociation of

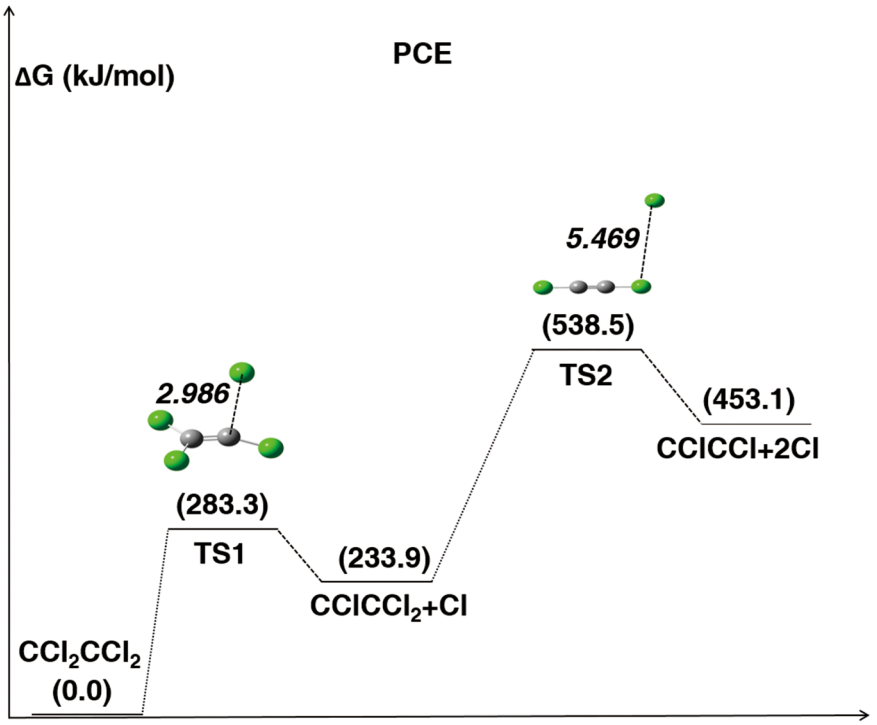

FIGURE 6 Profile of the Gibbs free energies for the dechlorination reactions of PCE in CID. Note, ΔG denotes relative Gibbs free energies, which are shown by the numbers in brackets; TS refers to transition state; bond lengths are in angstrom (Å) and indicated by the italic number

rotationally excited complexes. In addition, Petersen et al. reviewed the inverse Cl-KIEs observed in the study of Green et al.[14,20] and concluded that the large inverse Cl-KIEs were attributable to rotational predissociation and/or symmetry-induced KIEs according to the quantum calculation results. However, the near-threshold centrifugal effect cannot explain the fundamental mechanisms of the observed Cl-KIEs in our study, possibly because the cleaved C–Cl bonds are strong covalent bonds, which are less sensitive to angular momentum effects in comparison with loosely bounded systems such as chloroform/Cl^-. In the study of Green et al., the Cl-KIEs strongly relied on the particular isotopomers and showed increasing trends as CEs increased.[14] To the contrary, in our study, the Cl-KIEs were all isotopomer-independent and exhibited decreasing tendencies as the CEs increased (Figures 3 and 4). These differences may be also due to the different properties of the broken strong covalent bonds (C–Cl) and the dissociated loose coordinate bonds (C•••Cl^-).

The most notable phenomenon in our study was that the Cl-KIEs of DCM changed from large normal Cl-KIEs to extremely large inverse Cl-KIEs as the CEs increased from 0 to 60 eV, which has never been reported previously and is challenging to explain. To interpret this phenomenon, we refer to the theory in terms of competitive dechlorination reactions in EI-MS.[35,36] We take the reactions of $[CH_2{}^{35}Cl{}^{37}Cl]^{\bullet+} \rightarrow [CH_2{}^{35}Cl]^+$ (H) and $[CH_2{}^{35}Cl{}^{37}Cl]^{\bullet+} \rightarrow [CH_2{}^{37}Cl]^+$ (L) of DCM for example, which can be regarded as two isotope-competitive reactions during CID in MS/MS. As illustrated in Figure 7, the critical energy of reaction (H) is higher than that of reaction (L). Similarly, the internal energy threshold to generate just detectable product ion for the reaction (H) is higher than that for the reaction (L). At the internal energy of E_1, the rate constants of the two reactions reach equilibrium, that is, $k_{35Cl} = k_{37Cl}$ or Cl-KIE = 1. In the lower internal energy region ($E_{(L)}$-E_1), the rate constant of reaction (L) is higher than that of reaction (H), showing the Cl-KIE higher than unity. Because of the function of rate constant versus internal energy ($k(E)$) increases faster for the reaction (H) than for the reaction (L), the Cl-KIE gradually decreases to reach unity in the lower internal energy region and then begin to be under unity as the internal energy continues to increase in the higher internal energy region (>E_1). This type of competitive reactions is always related to the looseness and tightness of TSs,[37] and the $k(E)$ of the loose TS increases faster than that of the tight.[36] A loose TS means that the interacting fragments possess almost free rotations, while a tight TS has the fragments whose rotations are to some extent hindered.[38] This indicates that the loose TS has lower rotational barrier than the tight. Therefore, in the lower internal energy region, the reaction rate constants are dominated by critical energies, while in the higher internal energy region, the rate constants are controlled by rotational barriers. In this study, the TSs involving C–^{37}Cl may be slightly looser than those involving C–^{35}Cl, and therefore, the Cl-KIEs can decrease from higher than unity to lower than unity (namely, from normal to inverse). Accordingly, the phenomenon of normal and inverse Cl-KIEs observed in this study can be interpreted. However, more fundamental mechanisms involving atomic and electronic motions for the phenomenon need further in-depth exploration.

In this study, we discovered that the Cl-KIE ranges of DCM were evidently larger than those of TCE and PCE, which suggests that the Cl-KIE magnitudes of DCM were significantly larger than those of TCE and PCE at the same CEs (Figures 3 and 4). We infer that these differences might be owing to the C–Cl bond strength differences between DCM and the two chloroethylenes, given that the C–Cl bond strength of DCM (bond dissociation energy [BDE]: 338.0 ± 3.3 kJ/mol)

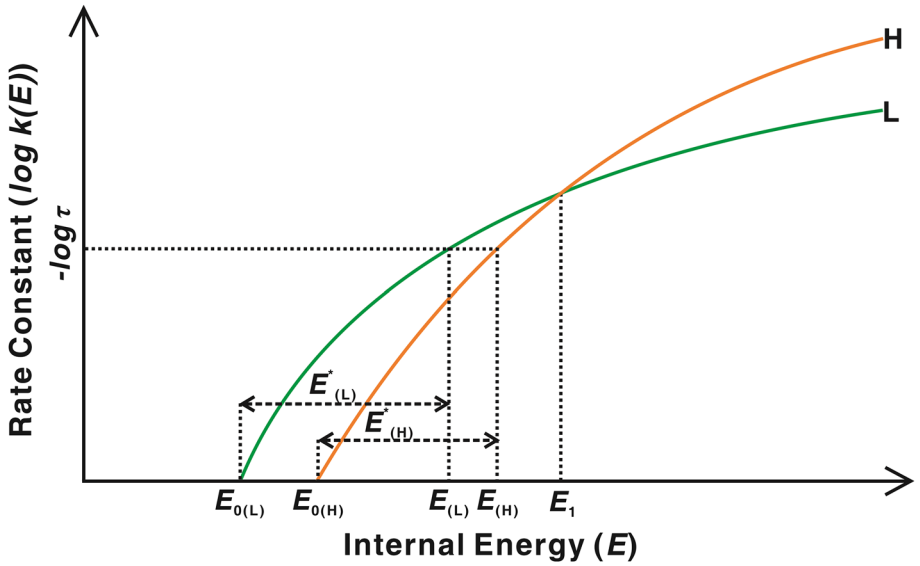

FIGURE 7 Illustration of the correlations between reaction rate constants (*log k(E)*) and internal energies (*E*) of two isotope-competitive dechlorination reactions in CID by GC-EI-MS/MS. Note, $E_{0(L)}$ and $E_{0(H)}$ denote the critical energies for the reactions $[CH_2{}^{35}Cl^{37}Cl]^{\bullet+} \rightarrow [CH_2{}^{37}Cl]^+$ (L) and $[CH_2{}^{35}Cl^{37}Cl]^{\bullet+} \rightarrow [CH_2{}^{35}Cl]^+$ (H), respectively; $E_{(L)}$ and $E_{(H)}$ correspond to the energy thresholds generating detectable ions of $[CH_2{}^{37}Cl]^+$ and $[CH_2{}^{35}Cl]^+$, respectively; $E^*_{(L)}$ and $E^*_{(H)}$ indicate the kinetic shifts for the reactions giving rise to detectable ions of $[CH_2{}^{37}Cl]^+$ and $[CH_2{}^{35}Cl]^+$, respectively; $-\log \tau$ represents the rate constant threshold where the product ions can just start to be detectable; E_1 is the internal energy of the precursor ion $[CH_2{}^{35}Cl^{37}Cl]^{\bullet+}$ at which the rate constants of the two reactions are equal. This diagram is referring to the literature[36]

is lower than those of the two chloroethylenes (BDEs ≥ 83.7 kJ/mol).[39,40] The reported dissociative photoionization onset energy of the reaction $CH_2Cl_2 \rightarrow [CH_2Cl]^+$ is 12.108 eV, and the onset energies positively correlate to bond strengths.[41] Therefore, it can be deduced that the onset energies of the reactions $C_2Cl_4 \rightarrow [C_2Cl_3]^+$ and $C_2HCl_3 \rightarrow [C_2HCl_2]^+$ are higher than that of the reaction $CH_2Cl_2 \rightarrow [CH_2Cl]^+$, which may be a reason for the discrepancy of the Cl-KIE magnitudes between DCM and the chloroethylenes. In addition, as shown in Figure 4, the Cl-KIEs derived from PCE by losing two Cl atoms were significantly higher than that from PCE by losing one atom. We deduce that the available internal energy (AIE) for breaking one C–Cl bond was higher than the mean of the AIEs for breaking two C–Cl bonds during CID, which is consistent with our quantum-chemical calculation results as shown in Figure 6. This difference in AIEs led to lower Cl-KIEs during the cleavage of one C–Cl bond than during the cleavages of two bonds because the Cl-KIEs decreased with the increase of CEs. The relative free energy (ΔG) in the reaction $[C_2Cl_4]^{\bullet+} \rightarrow [C_2Cl_3]^+$ (233.9 kJ/mol) is higher than a half of the reaction $[C_2Cl_4]^{\bullet+} \rightarrow [C_2Cl_2]^+$ (226.8 kJ/mol) (Figure 6), which leads to the relatively low Cl-KIEs in the former reaction than in the latter. In fact, the latter reaction comprises two stepwise reactions, that is, $[C_2Cl_4]^{\bullet+} \rightarrow [C_2Cl_3]^+$ and $[C_2Cl_3]^+ \rightarrow [C_2Cl_2]^+$. On the other hand, if the initial internal energies of the precursor ion $[C_2Cl_4]^{\bullet+}$ losing one Cl atom and that losing two Cl atoms are similar, the reaction $[C_2Cl_4]^{\bullet+} \rightarrow [C_2Cl_3]^+$ consumes partial internal energy (233.9 kJ/mol), leaving much less internal energy for the second reaction $[C_2Cl_3]^+ \rightarrow [C_2Cl_2]^+$ in comparison with the initial internal energies. Furthermore, the critical energies between the two steps of reactions are not sufficiently different (283.3 versus 304.6 kJ/mol). As a result, the second reaction $[C_2Cl_3]^+ \rightarrow [C_2Cl_2]^+$ can present higher Cl-KIEs compared with the first reaction $[C_2Cl_4]^{\bullet+} \rightarrow [C_2Cl_3]^+$, leading to the higher Cl-KIEs in the reaction $[C_2Cl_4]^{\bullet+} \rightarrow [C_2Cl_2]^+$ than in $[C_2Cl_4]^{\bullet+} \rightarrow [C_2Cl_3]^+$. We thus conclude that the Cl-KIEs during CID may depend on critical energies, bond strengths, AIEs, and TS looseness/tightness (or rotational barriers).

4 | CONCLUSIONS

In this study, we have systematically investigated the Cl-KIEs of DCM, TCE, and PCE in CID by GC–MS/MS. Unusually large inverse Cl-KIEs were observed for all the three organochlorines. Specifically for DCM, both intra-ion and inter-ion Cl-KIEs were explored, exhibiting both normal and inverse Cl-KIEs depending on CEs. The observed Cl-KIEs generally showed declining tendencies as the CEs increased from 0 to 60 eV, presenting evident CE-dependent features, but had no relationship with MS signal intensities, injection concentrations/volumes, and isotopologues' relative abundances. In a lower internal energy region, the Cl-KIEs are inferred to be dominated by critical energies, causing normal Cl-KIEs; while in a higher internal energy region, the Cl-KIEs are deduced to be controlled by looseness/tightness of TSs (or rotational barriers) that contribute to isotope-competitive reactions, thus leading to inverse Cl-KIEs. Overall, the Cl-KIEs may be dependent on critical energies, bond strengths, AIEs, and looseness/tightness of TSs. The findings of this study could be extended to revelation of Cl-KIEs in potodechlorination reactions and

KIEs of other elements in collision-induced and photoinduced dissociation reactions.

ACKNOWLEDGEMENTS

This study was financially supported by the National Natural Science Foundation of China (Grant No. 41603092, 41877365). The authors are grateful for the assistance from Dr. Liang Peng (School of Chemistry, South China Normal University, Guangzhou) in the quantum-chemical calculation for this work.

CONFLICT OF INTEREST

The authors declare that there are no conflicts of interest.

ORCID

Caiming Tang https://orcid.org/0000-0001-6951-4497

REFERENCES

1. Derrick PJ. Isotope effects in fragmentation. *Mass Spectrom Rev*. 1983;2(2):285-298.
2. Drahos L, Sztáray J, Vékey K. Theoretical calculation of isotope effects, kinetic energy release and effective temperatures for alkylamines. *Int J Mass Spectrom*. 2003;225(3):233-248.
3. Donchi KF, Uggerud E, Hvistendahl G, Derrick PJ. Isotope effects on kinetic energy release. Elimination of CH_4 from $[CH_3CHOH]^+$ and $[CH_2OCH_3]^+$. *Int J Mass Spectrom*. 1989;93(2):215-223.
4. Donchi KF, Brownlee RT, Derrick PJ. Kinetic isotope effects in the unimolecular gas-phase decomposition of propane radical cations. *Chem Commun*. 1980;22:1061-1062.
5. Ranasinghe YA, Glish GL. Intra-and intermolecular isotope effects for hydrogen loss from protonated aniline and the barrier to hydrogen transfer between the ring and substituent. *Int J Mass Spectrom*. 1999;190:295-302.
6. Ottinger CZ. Metastable ion decompositions in methane and the deuteromethanes. *Zeitschrift für Naturforschung a*. 1965;20(9):1232-1234.
7. Löhle U, Ottinger C. Metastable ions in the mass spectra of CD_3CH_3 and C_2H_6. *J Chem Phys*. 1969;51(7):3097-3104.
8. Tumas W, Foster RF, Pellerite MJ, Brauman JI. A stepwise mechanism for gas-phase unimolecular ion decompositions. Isotope effects in the fragmentation of tert-butoxide anion. *J Am Chem Soc*. 1987;109(4):961-970.
9. Tureček F. The use of kinetic isotope effects for the determination of internal energy distributions in isolated transient species in the gas phase. *Int J Mass Spectrom*. 2003;227(3):327-338.
10. Yamagaki T, Fukui K, Tachibana K. Analysis of glycosyl bond cleavage and related isotope effects in collision-induced dissociation quadrupole-time-of-flight mass spectrometry of isomeric trehaloses. *Anal Chem*. 2006;78(4):1015-1022.
11. Nielsen CB, Hammerum S. Secondary kinetic deuterium isotope effects. The C-C cleavage of labeled tetramethylethylenediamine radical cations—Who gets to keep the electron? *Int J Mass Spectrom*. 2017;413:92-96.
12. Norrman K, McMahon TB. Isotope effects in dissociation reactions of proton bound amine dimers in the gas phase. *Int J Mass Spectrom*. 1999;182:381-402.
13. Russell ME. Secondary isotope effects in the mass spectra of $C_2D_5OC_2H_5$ and $CD_3CH_2OC_2H_5$. *Org Mass Spectrom*. 1993;28:766-768.
14. Green JR, Cooks RG. Inverse heavy-atom kinetic isotope effects in chloroalkanes. *J Phys Chem A*. 2004;108:0039-10043.
15. Gozzo FC, Eberlin MN. Primary and secondary kinetic isotope effects in proton (H^+/D^+) and chloronium ion ($^{35}Cl^+/^{37}Cl^+$) affinities. *J Mass Spectrum*. 2001;36:1140-1148.
16. Augusti R, Zheng X, Turowski M, Cooks RG. Kinetic isotope and collision energy effects in the dissociation of chloride and bromide adducts of aliphatic alcohols, benzaldehyde, and 2, 4-pentanedione. *Aust J Chem*. 2003;56:415-421.
17. Tang C, Tan J, Shi Z, Fan Y, Yu Z, Peng X. Chlorine and bromine isotope fractionations of halogenated organic compounds in fragmentation by gas chromatography-electron ionization high resolution mass spectrometry. *J Chromatogr A*. 1603;2019:278-287.
18. Tang C, Peng L, Tan J, et al. Observation of varied characteristics of chlorine isotope effects of organochlorines in dechlorination reactions on different types of electron ionization mass spectrometers. *Int J Mass Spectrom*. 2020;447:116238.
19. Zakett D, Flynn RGA, Cooks RG. Chlorine isotope effects in mass spectrometry by multiple reaction monitoring. *J Phys Chem*. 1978;82:2359-2362.
20. Petersen AC, Sølling TI, Waters MD. Symmetry-induced kinetic isotope effects in the dissociation dynamics of $CHCl_3^+$ and $CHCl_4^-$. *Chem Phys*. 2018;515:375-380.
21. Lehman TA, Hass JR, Crow FW, Tomer KB, Pedersen LG. Isotope effects in collision-activated dissociations of simple ions. *Int J Mass Spectrom*. 1986;69:85-96.
22. Petersen AC, Hammerum S. The methylene chloride radical cation and its distonic isomers in the gas phase. *Int J Mass Spectrom*. 2001;210:403-415.
23. Petersen AC, Koerstz M, Mikkelsen KV, Sølling TI. Electronic predissociation in the dichloromethane cation $CH_2Cl_2^+$ electronic state 2A1. *J Phys Chem A*. 2019;123(18):4048-4056.
24. Tang C, Tan J, Xiong S, Liu J, Fan Y, Peng X. Chlorine and bromine isotope fractionation of halogenated organic pollutants on gas chromatography columns. *J Chromatogr A*. 2017;1514:103-109.
25. Tang C, Tan J. Simultaneous observation of concurrent two-dimensional carbon and chlorine/bromine isotope fractionations of halogenated organic compounds on gas chromatography. *Anal Chim Acta*. 2018;1039:172-182.
26. Frisch MJ, Trucks GW, Schlegel HB, et al. *Gaussian 09, Revision B.01*. Wallingford, CT: Gaussian, Inc; 2009.
27. Becke AD. Density-functional thermochemistry. III. The role of exact exchange. *J Chem Phys*. 1993;98:5648-5652.
28. Lee C, Yang W, Parr RG. Development of the Colle-Salvetti correlation-energy formula into a functional of the electron density. *Phys Rev B*. 1988;37:785-789.
29. Osterheld TH, Brauman JI. Infrared multiple photon dissociation of acetone radical cation. An enormous isotope effect with no apparent tunneling. *J Am Chem Soc*. 1992;114:7158-7164.
30. Marcus RA, Rice OK. The kinetics of the recombination of methyl radicals and iodine atoms. *J Phys Chem*. 1951;55:894-908.
31. Kassel LS. Bimolecular association reactions. *J Chem Phys*. 1937;5:922-924.
32. Rice OK. Energy exchange in unimolecular gas reactions. *J Am Chem Soc*. 1932;54:4558-4581.
33. Rice OK, Ramsperger HC. Theories of unimolecular gas reactions at low pressures. *J Am Chem Soc*. 1927;49:1617-1629.
34. Maccoll A, Baldwin MA. Letters to the editor. *J Mass Spectrom*. 1980;15:109-110.
35. Cooks RG, Howe I, Williams DH. Structure and fragmentation mechanisms of organic ions in the mass spectrometer. *Org Mass Spectrom*. 1969;2:137-156.
36. Brown P. Kinetic studies in mass spectrometry–VII: competing cleavage and rearrangement processes in molecular ion decomposition reactions. *Org Mass Spectrom*. 1970;3:1175-1186.

37. Chen JH, Hays JD, Dunbar RC. Competitive two-channel photodissociation of n-butylbenzene ions in the Fourier-transform ion cyclotron resonance mass spectrometer. *J Phys Chem*. 1984;88:4759-4764.
38. Truhlar DG, Garrett BC, Klippenstein SJ. Current status of transition-state theory. *J Phys Chem*. 1996;100:12771-12800.
39. Luo YR, Kerr JA. *Bond dissociation energies, CRC Handbook of Chemistry and Physics*. Oakville, Canada: Apple Academic Press Inc.. 2012:89.
40. Dávalos JZ, Notario R, Cuevas CA, Oliva JM, Saiz-Lopez A. Thermochemistry of halogen-containing organic compounds with influence on atmospheric chemistry. *Comput Theor Chem*. 2017;1099:36-44.
41. Harvey J, Tuckett RP, Bodi A. A halomethane thermochemical network from iPEPICO experiments and quantum chemical calculations. *J Phys Chem A*. 2012;116(39):9696-9705.

SUPPORTING INFORMATION

Additional supporting information may be found online in the Supporting Information section at the end of this article.

How to cite this article: Tang C, Tan J, Zhang P, Fan Y, Yu Z, Peng X. Energy-dependent normal and unusually large inverse chlorine kinetic isotope effects of simple chlorohydrocarbons in collision-induced dissociation by gas chromatography-electron ionization-tandem mass spectrometry. *J Mass Spectrom*. 2020;55:e4521. https://doi.org/10.1002/jms.4521